

Laser cooling and trapping of $^{224}\text{Ra}^+$

M. Fan,^{1,*} Roy A. Ready,¹ H. Li,¹ S. Kofford,¹ R. Kwapisz,¹ C. A. Holliman,¹
M. S. Ladabaum,¹ A. N. Gaiser,^{2,3} J. R. Griswold,⁴ and A. M. Jayich¹

¹*Department of Physics, University of California, Santa Barbara, California 93106, USA*

²*Department of Chemistry, Michigan State University, East Lansing, MI 48824 USA*

³*Facility for Rare Isotope Beams, Michigan State University, East Lansing, MI 48824 USA*

⁴*Radioisotope Science and Technology Division, Oak Ridge National Laboratory, Oak Ridge, TN 37830 USA*

(Dated: August 2, 2023)

We report the first laser cooling and trapping of $^{224}\text{Ra}^+$ ions. This was realized via the first loading of radium into an ion trap with two step photoionization. A robust source for ^{224}Ra atoms, 3.6 day half-life, was realized with an effusive oven containing ^{228}Th , 1.9 year half-life, which continuously generates ^{224}Ra via its α -decay. We characterized the efficacy of this source and found that after depleting built up radium the thorium decay provides a continuous source of radium atoms suitable for ion trapping. The vacuum system has been sealed for more than six months and continues to trap ions on demand. We also report a measurement of the $^{224}\text{Ra } 7s^2 \ ^1S_0 \rightarrow 7s7p \ ^1P_1$ transition frequency: 621 043 830(60) MHz, which is helpful for efficient photoionization. With this measurement and previous isotope shift measurements [1] we recommend a correction to the same transition in ^{226}Ra : 621 037 830(60) MHz, which is 660 MHz from the accepted value.

INTRODUCTION

Radium, the heaviest alkaline earth element, has favorable electronic properties for laser cooling and trapping in both neutral and singly ionized forms [2, 3]. Ra^+ has a narrow linewidth electric quadrupole (E2) transition which is advantageous for trapped ion optical clocks [4, 5]. The clock operates with wavelengths that are compatible with integrated photonic technologies which make Ra^+ appealing for a transportable optical clock. Certain isotopes of radium have an octupole deformed nucleus which when paired with nuclear spin, such as ^{225}Ra ($I = 1/2$), enhances sensitivity to time-reversal symmetry violations [6]. A challenge with radium is that there are no stable isotopes. The longest lived, ^{226}Ra ($I = 0$), has a 1600 year half-life, while ^{225}Ra has only a 15 day half-life. For all radium isotopes radioactivity limits their use to small quantities.

Previous atomic and molecular experiments used a variety of mechanisms to work with various radium isotopes: Spectroscopy of trapped $^{209-214}\text{Ra}^+$ ions was done at the TRI μ P nuclear facility where radium atoms were produced when a lead beam impinged on a carbon target [7]. An optical atomic clock was demonstrated with a $^{226}\text{Ra}^+$ ion where the Ra^+ was produced via laser ablation of a radium chloride target in the vacuum system [5]. The atomic electric dipole moment of neutral ^{225}Ra was measured in an optical dipole trap where ^{225}Ra was directly loaded into an effusive oven and heated out for laser cooling and trapping [6]. Radium isotopes were produced at CERN by using 1.4 GeV protons to irradiate a uranium carbide target which was then heated to release radium atoms to form RaF for spectroscopy [8]. When working with all but ^{226}Ra these techniques require specialized facilities and or breaking vacuum on timescales incommensurate with typical atomic and molecular ex-

periments. Fortunately, thorium may be used as a generator to continuously produce *in vacuo* ^{224}Ra , ^{226}Ra and the desirable ^{225}Ra isotope, relieving the need for nuclear facilities or opening vacuum systems. This method was used for spectroscopy of neutral ^{225}Ra from an effusive oven [9, 10].

Thorium has a vapor pressure that is more than a trillion times lower than radium [11]; therefore when an oven is heated it will produce a radium beam while all but a negligible quantity of thorium will remain in the oven. An oven based on this mechanism should provide radium for several thorium half-lives. We use an effusive oven based on this mechanism to realize the first photoionization loading of radium ions into an ion trap and the first laser cooling of $^{224}\text{Ra}^+$ ions. Radium-224, half-life 3.6 days [12], is continuously produced by the α -decay of ^{228}Th , half-life 1.9 years, in the oven's crucible. The effectiveness of the oven for ion trap experiments is demonstrated by measuring the trapping rates for several oven temperatures. When the oven is depleted of radium that has built up over several days the continual decay of thorium generates a sufficient radium flux for ion trapping.

OVEN DESIGN

Effusive atomic ovens are a common means to generate atomic beams for laser cooling and trapping of both neutral and ionized atoms [13, 14]. The oven reported here is based on an effusion cell design commonly used for molecular beam epitaxy (MBE) [15]. The effusion cell has heater wires that can heat a titanium crucible up to 1470 K. The crucible's interior is a 59 mm long cylinder with a 7 mm diameter. The crucible cap has a 12.7 mm long, 2 mm diameter aperture, see Fig. 1. We

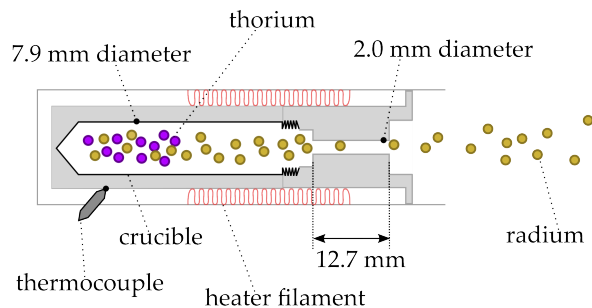


FIG. 1. A schematic of the effusive oven. A titanium crucible was loaded with ^{228}Th (purple circles). The crucible is resistively heated to emit a thermal beam of radium atoms (gold circles). The crucible's temperature is measured with a thermocouple in contact with its outer surface.

transferred 40(20) μCi of $^{228}\text{Th}(\text{NO}_3)_4$ in 0.1 M HNO_3 into the crucible and dried the solution in the oven by heating the crucible with a hot plate to ~ 350 K. Once dried, we added ~ 1 mg of strontium, attached the cap, put the crucible in the effusion cell, and installed it to a vacuum chamber. Initially, a strontium beam from the heated oven was used for laser alignment and ion trap testing. This strontium may play a role in reducing radium compounds which might form due to reactions with contaminants.

LASER COOLING AND TRAPPING

Photoionization (PI) and subsequent laser cooling and trapping of $^{224}\text{Ra}^+$ was realized with the trap depicted in Fig. 2(a). The trap is a linear Paul trap, described in [3]; the diagonal radio-frequency (rf) electrodes are separated by 6 mm and the end cap electrodes by 15 mm. The trap center is 44 mm from the oven aperture and the rf drive frequency is 990 kHz. Permanent magnets generate a 5.0(5) Gauss static magnetic field at approximately 90° with respect to the laser cooling beams.

Radium atoms from the oven are photoionized in a two stage process, see Fig. 2(b). This process is similar to the scheme used for other alkaline earth atoms [16, 17]. First, neutral radium is excited on the $^1\text{S}_0 \rightarrow ^1\text{P}_1$ transition with 1.1 mW of 483 nm light. A photoionizing beam then drives the population from the $^1\text{P}_1$ level to the continuum with 1 mW of 450 nm light. The photoionizing beam waist is at the trap center and is approximately $150 \mu\text{m}$. Laser cooling is realized with a 468 nm cooling laser red detuned from the $7s \ ^2\text{S}_{1/2} \rightarrow 7p \ ^2\text{P}_{1/2}$ transition and a 1079 nm repump laser that drives the $6d \ ^2\text{D}_{3/2} \rightarrow 7p \ ^2\text{P}_{1/2}$ transition, see Fig. 2(c). Scattered 468 nm light is collected by the imaging system and focused onto a photomultiplier tube (PMT) and a camera [3].

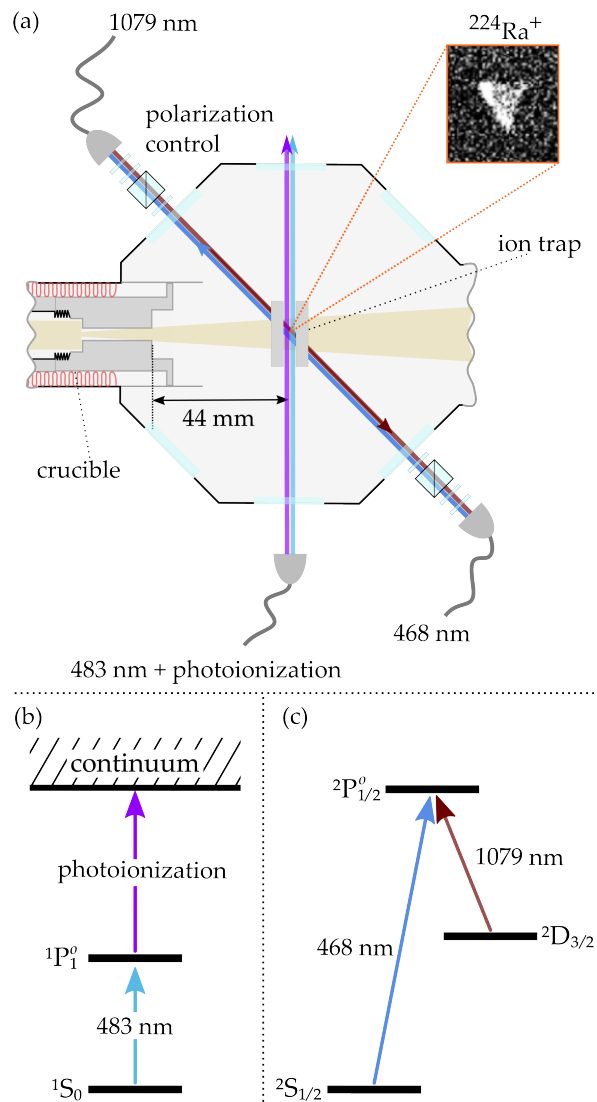


FIG. 2. (a) A schematic of the apparatus for photoionization, laser cooling and trapping of $^{224}\text{Ra}^+$. The trap is a linear Paul trap depicted by two rf rods. The effusive oven geometry is given in Fig. 1. (b) The transitions used for photoionization of ^{224}Ra . 405 nm, 422 nm, and 450 nm lasers were tested on the $^1\text{P}_1$ transition to the continuum. (c) The $^{224}\text{Ra}^+$ level structure with the laser cooling transitions highlighted.

Three PI laser wavelengths (405 nm, 422 nm, and 450 nm) were tested for the second photoionization step. These three wavelengths are all above the 458 nm ionization energy threshold from the $^1\text{P}_1$ state. The number of ^{224}Ra atoms photoionized and detected in the trap per minute (the ion capture rate) was measured for each wavelength. The three PI wavelengths produced comparable ion capture rates for similar powers. In practice, we used 450 nm light because it had the most available power (~ 1 mW at the trap).

Rydberg autoionization was explored using 461 nm and 468 nm lasers as the second PI stage to excite Rydberg

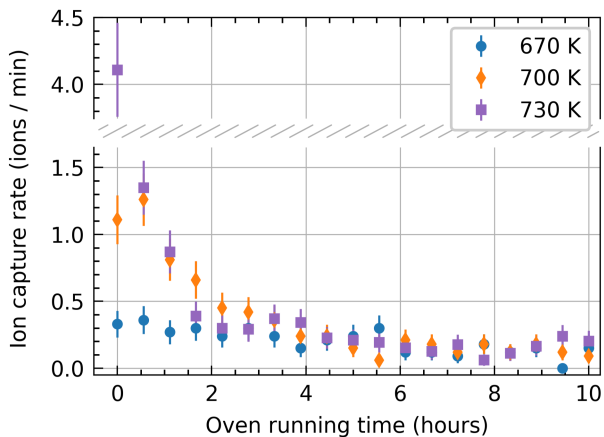


FIG. 3. $^{224}\text{Ra}^+$ ion capture rates at different oven temperatures as a function of time. The 450 nm photoionization laser has 1 mW optical power and a 150 μm beam waist at the ion trap.

states. The PI rate with 461 nm light was lower than that with 450 nm, and no ions were trapped when using 468 nm light. We verified that radium could still be ionized and trapped with the 450 nm PI light before, during, and after the Rydberg tests.

We characterized the reliability and longevity of the oven source by measuring the ion capture rate for extended periods of operation. The ion capture rate was determined by an automated process which monitored PMT counts from laser cooled radium ions. When the PMT counts exceeded a detection threshold, the trap's rf power was switched off to dump the ion and then turned back on to trap the next ion. The time between turning on the rf and loading a new ion was recorded to determine the ion capture rate. The photoionization beams were applied continuously. The ion capture rate at several oven temperatures as a function of time is shown in Fig. 3. The high initial capture rate, a consequence of the flux of radium atoms that have built up prior to turning on the oven, increases rapidly with oven temperature. On the order of 10^{11} radium atoms accumulate in one ^{224}Ra half-life [18]. After the initial surge, the continual decay of thorium is sufficient to maintain a flux of radium atoms for trapping. A steady state capture rate of $\sim 0.13(1)$ ions/min is reached after approximately three hours for each oven operating temperature that was tested. At higher temperatures, the steady state capture rate increases due to a combination of increased rates of radium desorption from surfaces and effusion out of the crucible's titanium walls [19, 20].

NEUTRAL RA-224 SPECTROSCOPY

The $7s^2\ ^1S_0 \rightarrow 7s7p\ ^1P_1$ ($^1S_0 \rightarrow ^1P_1$) radium transition at 483 nm is useful for photoionization loading of

radium into ion traps. The $^1S_0 \rightarrow ^1P_1$ transition was first measured for ^{226}Ra by Rasmussen in 1933 [21]. Subsequent spectroscopy of this transition has been done for ^{226}Ra and ^{225}Ra [10, 22]. We measured the $^1S_0 \rightarrow ^1P_1$ transition of ^{224}Ra frequency and compared our value with the previous results using the isotope shift measurements of Wendt, *et al.* [1]. Saturated absorption spectroscopy of molecular tellurium ($^{130}\text{Te}_2$) was used as a frequency reference for the ^{224}Ra spectroscopy [10].

For saturated absorption spectroscopy, two parallel 483 nm probe beams and a counter-propagating pump beam which overlaps with one of the probe beams are passed through a cell containing $^{130}\text{Te}_2$ at 870(20) K. All three beams are derived from a single laser. The probes, each 60(10) μW , are collected on a balanced photodiode and their signals are subtracted. The pump beam, shifted 80 MHz by an acousto-optic modulator (AOM) relative to the probe light, has 1.3(1) mW of power and a 0.8(1) mm beam waist at the center of the $^{130}\text{Te}_2$ cell. The AOM serves as a shutter for the pump beam, turning it on and off at a modulation frequency of 10 kHz. The same 10 kHz modulation frequency is mixed with the split photodiode output with a lock-in amplifier to measure the Te_2 spectrum.

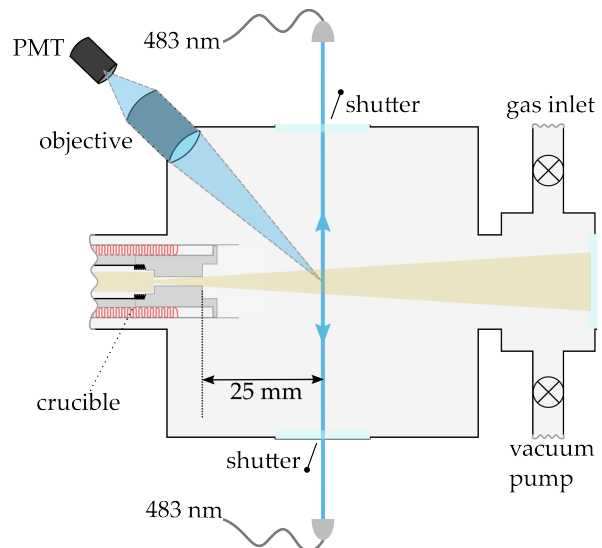


FIG. 4. A schematic of the vacuum apparatus used for neutral spectroscopy of ^{224}Ra . The setup uses an effusive oven with the same geometry as in Fig. 1. A gas inlet valve allows for the introduction of gas, such as argon, into the chamber. A pair of counter-propagating 483 nm beams are perpendicular to the atomic beam. A fraction of the fluorescence from atoms excited on the $^1S_0 \rightarrow ^1P_1$ transition is collected by an imaging objective and focused onto a PMT.

Spectroscopy of ^{224}Ra was done in the vacuum apparatus depicted in Fig. 4. A thermal beam of ^{224}Ra atoms is generated by heating the oven to 880(10) K. Two counter-propagating 483 nm laser beams (each 1.5(1) mW) are

perpendicular to the radium beam 25 mm from the oven aperture. The beam waists are 3.4(1) mm. The geometry is chosen to minimize the effect of Doppler broadening. Radium atoms are excited on the $^1S_0 \rightarrow ^1P_1$ transition and scattered light is collected by an imaging objective on to a PMT.

The 483 nm laser frequency is scanned continuously while the two counter propagating beams are alternately shuttered and the two spectra are recorded. The reported frequency of the $^{224}\text{Ra } ^1S_0 \rightarrow ^1P_1$ transition is the average frequency of both spectra using a wavemeter (10 MHz resolution) [23] calibrated with the $^{130}\text{Te}_2$ reference line #0, see Fig. 5. The fit uncertainties for the ^{224}Ra and $^{130}\text{Te}_2$ transitions are their fitted half-width-half-maximum values which account for model imperfections. Wavemeter drift is determined from the difference between the $^{130}\text{Te}_2$ saturated absorption spectrum measured before and after the ^{224}Ra spectroscopy. The observed wavemeter drift within the measurement time of ~ 2 hours is 2 MHz. The latter $^{130}\text{Te}_2$ spectrum and the ^{224}Ra spectra are shown in Fig. 5. Imperfect alignment of the 483 nm beams results in a 1(9) MHz first-order Doppler shift. The reported $^1S_0 \rightarrow ^1P_1$ transition frequency for ^{224}Ra is 621 043 830(60) MHz.

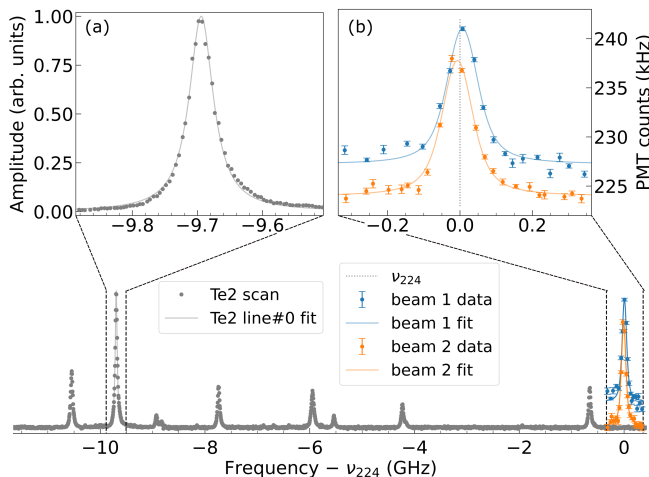


FIG. 5. Spectroscopy of the $^{224}\text{Ra } 7s^2 ^1S_0 \rightarrow 7s7p ^1P_1$ transition and saturated absorption spectroscopy of $^{130}\text{Te}_2$ peaks covering line#-1 to line#6 as labeled in [10], where ν_{224} is our measured ^{224}Ra transition frequency. The amplitude of the $^{130}\text{Te}_2$ saturated absorption signal is normalized to Te_2 line#0. The measured $^{224}\text{Ra } ^1S_0 \rightarrow ^1P_1$ transition frequency is calibrated from the Te_2 spectrum. The difference in peak height between beam 1 (blue) and beam 2 (orange) is due to the decay in atomic flux during the measurement. Inset (a) shows the Lorentzian fit of the Doppler-free Te_2 line #0. Inset (b) shows the Voigt fit of the fluorescence from the thermal ^{224}Ra beam.

We determine the $^{226}\text{Ra } ^1S_0 \rightarrow ^1P_1$ transition frequency: 621 037 830(60) MHz, by the isotope shifts of ^{224}Ra and ^{226}Ra with respect to ^{214}Ra [1]. There is a 660 MHz discrepancy between our value for the $^1S_0 \rightarrow ^1P_1$

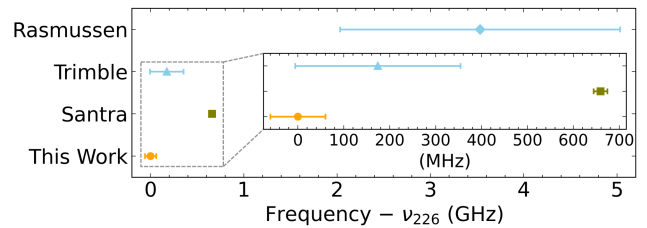


FIG. 6. A comparison of the reported $^{226}\text{Ra } 7s^2 ^1S_0 \rightarrow 7s7p ^1P_1$ transition frequencies where ν_{226} is our value. Frequencies reported by Rasmussen [21] and Trimble *et al.* [22] are direct measurements. The frequency reported by Santra *et al.* [10] is an isotope shifted value from their measurement of the ^{225}Ra transition frequency.

transition frequency and the value reported in [24], see Fig. 6.

NULL RESULTS

Short-lived radioisotopes are challenging to work with, particularly due to the difficulty of producing a sufficient atom flux for neutral spectroscopy and ion trapping. Radium poses further difficulties as it is reactive. Different techniques were tested in the neutral spectroscopy setup of Fig. 4 with indeterminate results or uncertain effectiveness, some of which are described here as paths for future exploration.

Argon gas with a pressure of ~ 100 Torr was flowed through the neutral spectroscopy apparatus in an effort to slow the radium atoms after nuclear decay and prevent them from becoming deeply buried in the titanium walls of the crucible [25]. No increase in PMT counts on the $^1S_0 \rightarrow ^1P_1$ transition was observed.

We also investigated reducing agents. When ^{228}Th was loaded into the crucible without any reducing agents no $^1S_0 \rightarrow ^1P_1$ transition peak was observed. After adding in ~ 1 mg of strontium, 200 mg Zr powder, and 50 mg BaCO_3 to the crucible to reduce radium compounds [10], there was an increase in the neutral radium spectroscopy signal compared to when only strontium was used. However, it is unclear if the lack of signal without reducing agents was due to a low pressure of reactive background gas molecules rather than the lack of reducing agents. The pressure of the neutral spectroscopy chamber ($\sim 10^{-5}$ Torr with an oven temperature of 880(10) K) was three orders of magnitude higher than that of the ion trapping apparatus. At the lower pressures achieved in the ion trap, reducing agents may not be necessary.

CONCLUSION

This work lowers the barrier to using the short-lived ^{224}Ra isotope in cold atom experiments. An effusive

oven based on the decay of thorium is a reliable source of radium atoms for ion trapping experiments, and could be used for cold neutral atom experiments depending on atom number requirements and acceptable activity. The source efficiency may be increased with more advanced oven nozzle geometries [26]. An oven based on the same principle may be used to laser cool and trap ^{225}Ra ions, produced via the decay of ^{229}Th (7825 year half-life [27]), or ^{226}Ra ions, produced via the decay of ^{230}Th (75 thousand year half-life). Such ovens are robust to radium depletion, *e.g.* due to overheating the oven, as radium is continuously repopulated by thorium.

ACKNOWLEDGEMENTS

We thank Chris Palmstrøm, Dave DeMille, Bodhadiya Santra and Lorenz Willmann for helpful discussions, Craig B. for help with the MBE oven configuration, and Dave Patterson for lending a 461 nm laser. We thank Chris Greene and Miguel A. Alarcón for guiding calculations. MF and HL were supported by DoE award DE-SC0022034. SK was supported by ONR Grant N00014-21-1-2597. Other members of UCSB were supported by NSF award PHY-2146555, NIST award 60NANB21D185, the Heising-Simons Foundation, the W.M. Keck Foundation, and the Eddleman Center. ANG acknowledges the support of startup funds and Michigan State University. The isotope used in this research was supplied by the U.S. Department of Energy Isotope Program, managed by the Office of Isotope R&D and Production.

* mingyufan212@gmail.com

- [1] K. Wendt, S. A. Ahmad, W. Klempt, R. Neugart, E. W. Otten, and H. H. Stroke, *Zeitschrift für Physik D Atoms, Molecules and Clusters* **4**, 227 (1987).
- [2] J. R. Guest, N. D. Scielzo, I. Ahmad, K. Bailey, J. P. Greene, R. J. Holt, Z.-T. Lu, T. P. O'Connor, and D. H. Potterveld, *PRL* **98**, 093001 (2007).
- [3] M. Fan, C. A. Holliman, A. L. Wang, and A. M. Jayich, *PRL* **122**, 223001 (2019).
- [4] O. O. Versolato, L. W. Wansbeek, K. Jungmann, R. G. E. Timmermans, L. Willmann, and H. W. Wilschut, *PRA* **83**, 043829 (2011).
- [5] C. A. Holliman, M. Fan, A. Contractor, S. M. Brewer, and A. M. Jayich, *PRL* **128**, 033202 (2022).
- [6] R. H. Parker, M. R. Dietrich, M. R. Kalita, N. D. Lemke, K. G. Bailey, M. Bishop, J. P. Greene, R. J. Holt, W. Korsch, Z.-T. Lu, P. Mueller, T. P. O'Connor, and J. T. Singh, *Phys. Rev. Lett.* **114**, 233002 (2015).
- [7] G. S. Giri, O. O. Versolato, J. E. van den Berg, O. Böll, U. Dammalapati, D. J. van der Hoek, K. Jungmann, W. L. Kruithof, S. Müller, M. Nuñez Portela, C. J. G. Onderwater, B. Santra, R. G. E. Timmermans, L. W. Wansbeek, L. Willmann, and H. W. Wilschut, *PRA* **84**, 020503 (2011).
- [8] R. F. Garcia Ruiz, R. Berger, J. Billowes, C. L. Binnersley, M. L. Bissell, A. A. Breier, A. J. Brinson, K. Chrysalidis, T. E. Cocolios, B. S. Cooper, K. T. Flanagan, T. F. Giesen, R. P. de Groote, S. Franchoo, F. P. Gustafsson, T. A. Isaev, A. Koszorus, G. Neyens, H. A. Perrett, C. M. Ricketts, S. Rothe, L. Schweikhard, A. R. Vernon, K. D. A. Wendt, F. Wienholtz, S. G. Wilkins, and X. F. Yang, *Nature* **581**, 396 (2020).
- [9] B. Santra, *Precision spectroscopy of neutral radium: towards searches for permanent electric dipole Electric*, Ph.D. thesis, University of Groningen (2013).
- [10] B. Santra, U. Dammalapati, A. Groot, K. Jungmann, and L. Willmann, *Phys. Rev. A* **90**, 040501 (2014).
- [11] W. Haynes, *CRC Handbook of Chemistry and Physics, 96th Edition* (CRC Press, 2015).
- [12] D. E. Bergeron, S. M. Collins, L. Pibida, J. T. Cessna, R. Fitzgerald, B. E. Zimmerman, P. Ivanov, J. D. Keightley, and E. Napoli, *Applied Radiation and Isotopes* **170**, 109572 (2021).
- [13] K. J. Ross and B. Sonntag, *Review of Scientific Instruments* **66**, 4409 (1995), <https://doi.org/10.1063/1.1145337>.
- [14] U. Dammalapati, I. Norris, L. Maguire, M. Borkowski, and E. Riis, *Measurement Science and Technology* **20**, 095303 (2009).
- [15] The specific MBE oven used in this work was an E-Science Model No. EC-010-275-0800-HL.
- [16] D. M. Lucas, A. Ramos, J. P. Home, M. J. McDonnell, S. Nakayama, J.-P. Stacey, S. C. Webster, D. N. Stacey, and A. M. Steane, *PRA* **69**, 012711 (2004).
- [17] K. Vant, J. Chiaverini, W. Lybarger, and D. J. Berkeland, *Photoionization of strontium for trapped-ion quantum information processing* (2006), arXiv:quant-ph/0607055 [quant-ph].
- [18] A. Malins and T. Lemoine, *Journal of Open Source Software* **7**, 3318 (2022).
- [19] G. Beyer, E. Hagebø, A. Novgorodov, and H. Ravn, *Nuclear Instruments and Methods in Physics Research Section B: Beam Interactions with Materials and Atoms* **204**, 225 (2003), 14th International Conference on Electromagnetic Isotope Separators and Techniques Related to their Applications.
- [20] D. Melconian, M. Trinczek, A. Gorelov, W. P. Alford, J. A. Behr, J. M. D'Auria, M. Dombisky, U. Giesen, K. P. Jackson, T. B. Swanson, and W. Wong, *Nuclear Instruments and Methods in Physics Research Section A: Accelerators, Spectrometers, Detectors and Associated Equipment* **538**, 93 (2005).
- [21] E. Rasmussen, *Zeitschrift für Physik* **86**, 24 (1933).
- [22] W. L. Trimble, I. A. Sulai, I. Ahmad, K. Bailey, B. Graner, J. P. Greene, R. J. Holt, W. Korsch, Z.-T. Lu, P. Mueller, and T. P. O'Connor, *Phys. Rev. A* **80**, 054501 (2009).
- [23] HighFinesse WS8.
- [24] U. Dammalapati, K. Jungmann, and L. Willmann, *J. Phys. Chem. Ref. Data* **45**, 013101 (2016).
- [25] L. von der Wense, B. Seiferle, M. Laatiaoui, J. B. Neumayr, H.-J. Maier, H.-F. Wirth, C. Mokry, J. Runke, K. Eberhardt, C. E. Düllmann, N. G. Trautmann, and P. G. Thirolf, *Nature* **533**, 47 (2016).
- [26] R. Senaratne, S. V. Rajagopal, Z. A. Geiger, K. M. Fujiwara, V. Lebedev, and D. M. Weld, *Review of Scientific Instruments* **86**, 023105 (2015).

- [27] R. M. Essex, J. L. Mann, R. Collé, L. Laureano-Perez, M. E. Bennett, H. Dion, R. Fitzgerald, A. M. Gaffney, A. Gourgiotis, A. Hubert, K. G. W. Inn, W. S. Kinman, S. P. Lamont, R. Steiner, and R. W. Williams, *Journal of Radioanalytical and Nuclear Chemistry* **318**, 515 (2018).